



**HAL**  
open science

# High-intensity rainfall following drought triggers extreme nutrient concentrations in a small agricultural catchment

Rémi Dupas, Mikael Fauchaux, Tristan Senga Kiessé, Andrés Casanova,  
Nicolai Brekenfeld, Ophélie Fovet

► **To cite this version:**

Rémi Dupas, Mikael Fauchaux, Tristan Senga Kiessé, Andrés Casanova, Nicolai Brekenfeld, et al.. High-intensity rainfall following drought triggers extreme nutrient concentrations in a small agricultural catchment. *Water Research*, 2024, 264, pp.122108. 10.1016/j.watres.2024.122108 . hal-04669650

**HAL Id: hal-04669650**

**<https://hal.science/hal-04669650v1>**

Submitted on 9 Aug 2024

**HAL** is a multi-disciplinary open access archive for the deposit and dissemination of scientific research documents, whether they are published or not. The documents may come from teaching and research institutions in France or abroad, or from public or private research centers.

L'archive ouverte pluridisciplinaire **HAL**, est destinée au dépôt et à la diffusion de documents scientifiques de niveau recherche, publiés ou non, émanant des établissements d'enseignement et de recherche français ou étrangers, des laboratoires publics ou privés.



Distributed under a Creative Commons Attribution 4.0 International License



# High-intensity rainfall following drought triggers extreme nutrient concentrations in a small agricultural catchment

Rémi Dupas<sup>\*</sup>, Mikaël Faucheux, Tristan Senga Kiessé, Andrés Casanova, Nicolai Brekenfeld, Ophélie Fovet

Institut Agro, UMR1069 SAS, INRAE, 65 rue de Saint-Brieuc, Rennes, CEDEX 35000, France

## ARTICLE INFO

### Keywords:

Climate change  
Extreme event  
Nutrient  
Storm  
Agricultural catchment

## ABSTRACT

The profound influence of climate change on the hydrological cycle raises concerns about its potential impacts on water quality, particularly in agricultural catchments. Here, we analysed 200 storm events monitored for nitrate and total phosphorus (TP) at sub-hourly intervals from 2016 to 2023 in the Kervidy-Naizin catchment (north-western France). Using Extreme Value theory, we identified storm events with extreme concentrations and compared their hydroclimatic characteristics to those of non-extreme events. We hypothesised that extreme concentration events occurred under extreme hydroclimatic conditions, which are projected to become more frequent in the future. The extreme events identified showed dilution patterns for nitrate, with concentrations decreasing by up to 41 %, and accretion patterns for TP, with concentrations increasing by up to 1400 % compared to non-extreme events. Hydroclimatic conditions during extreme concentration events were characterised by high rainfall intensities and low antecedent discharge, but no particular conditions for mean discharge. During non-extreme events, nitrate concentration-discharge relationships exhibited primarily clockwise hysteresis, whereas TP displayed an equal mix of clockwise and anticlockwise loops. In contrast, extreme events showed more anticlockwise hysteresis for nitrate and weak hysteresis for TP. We interpreted these dynamics and their hydroclimatic controls as the result of infiltration-excess overland flow diluting nitrate-rich groundwater and exporting large amounts of TP during intensive rainfall events following droughts, while groundwater fluctuations in the riparian zone and streambed remobilization control nutrient exports during non-extreme events. Given the increasing frequency and intensity of hydroclimatic extremes, such retrospective analyses can provide valuable insights into future nutrient dynamics in streams draining agricultural catchments.

## 1. Introduction

Climate change impacts ecosystems in many ways, including through alteration of the hydrological cycle (Pörtner et al., 2022). Global hydrological models agree that climate change leads to an overall increase in the seasonality of river discharge and more frequent hydrological extremes (Eisner et al., 2017; Hirabayashi et al., 2008; van Vliet et al., 2013). In contrast, climate change impacts on water quality are highly dependent on the type of pollutant, water body and catchment characteristics (Mosley, 2015; Li et al., 2024). A recent review of 965 case studies published from 2000 to 2022 found that droughts and heatwaves degraded water quality in 68 % of reported cases (Van Vliet et al., 2023). The same review found that floods degraded water quality in 51 % of reported cases, while 56 % of the studies that considered overall climate change impacts reported a degradation (Van Vliet et al., 2023).

For nutrients, droughts and heatwaves tend to increase concentrations in environments with point sources due to the decreasing capacity of rivers to dilute concentrations (Abily et al., 2021), while they tend to decrease concentrations in environments with dominant diffuse sources due to decreasing catchment delivery to rivers and increasing retention (Mosley, 2015; Van Vliet et al., 2023; Li et al., 2024). During floods, the concentration of nutrients in particulate form such as phosphorus (P) tend to increase due to increasing erosion and remobilization of in-stream sources (Bieroza and Heathwaite, 2015; Dupas et al., 2015; Mellander et al., 2015), while the response of dissolved constituents is more varied (van Vliet et al., 2023). For example, nitrate-poor water from shallow flowpaths may dilute nitrate-rich groundwater during floods (Dupas et al., 2016; Fovet et al., 2018a; Melland et al., 2012). Quantifying the overall long-term effect of climate change on water quality is particularly challenging, whether using retrospective

<sup>\*</sup> Corresponding author.

E-mail address: [remi.dupas@inrae.fr](mailto:remi.dupas@inrae.fr) (R. Dupas).

<https://doi.org/10.1016/j.watres.2024.122108>

Received 22 March 2024; Received in revised form 2 July 2024; Accepted 3 July 2024

Available online 25 July 2024

0043-1354/© 2024 The Author(s). Published by Elsevier Ltd. This is an open access article under the CC BY license (<http://creativecommons.org/licenses/by/4.0/>).

approaches or prospective modelling approaches. Retrospective approaches can estimate long-term trends in concentrations, but they have difficulty distinguishing direct effects of climate change from those of simultaneous changes in land use and management (Strohmenger et al., 2020). Conversely, prospective modelling approaches experience high uncertainties in defining future land-use and management scenarios, among other sources of uncertainty (Jin et al., 2015).

The present study contributes to the knowledge of the effects of climate extremes, specifically extreme storm events, on nutrient concentrations and fluxes in intensively farmed catchments. Unlike most of the literature on nutrient export dynamics during storm events, which increased greatly after the development of affordable high-frequency measurement techniques (Bierzoa et al., 2023; Rode et al., 2016; Speir et al., 2023), we specifically focused on extreme concentration events that may become more frequent in the future along with hydroclimatic extremes. The Kervidy-Naizin catchment in northwestern France is particularly suitable for this analysis because 25 years of research there have provided knowledge on hydrological controls of its nutrient concentrations and fluxes (Fovet et al., 2018b; Gascuel-Oudoux et al., 2018). This research included analysis of nutrient dynamics during storm events (e.g., Aubert et al. 2013; Dupas et al. 2015; Fovet et al. 2018a; Strohmenger et al. 2020), which we compared to nutrient dynamics during extreme events analysed in the present study. The Kervidy-Naizin catchment has also been compared to other agricultural catchments in north-western Europe to confirm that, despite differences in concentrations, nutrient dynamics during storm events were representative of this type of context (Bol et al., 2018; Dupas et al., 2017; Mellander et al., 2018). Previous studies in Kervidy-Naizin and similar catchments have shown that nutrient dynamics during storm events tend to show an accretion pattern for P forms and a dilution pattern for nitrate. Concentration-discharge hysteresis patterns are usually clockwise for particulate P, suggesting proximal sources and transfer through infiltration-excess overland flow, and anticlockwise for dissolved P, suggesting more distal sources and transfer through saturation-excess runoff or subsurface pathways in the riparian zone (Dupas et al., 2015). Hysteresis patterns for nitrate are usually clockwise due to the contribution of nitrate-poor riparian water in the falling limb of the hydrograph, although with high variability depending on hydrological conditions (Fovet et al., 2018a; Lloyd et al., 2016b; Musolff et al., 2021). In other climate, land-use and soil contexts, nutrient concentration-discharge relationships can have a variety of hysteresis and slope patterns, and they usually vary depending on seasonal and hydrological conditions (e.g., Kincaid et al. 2020; Ockenden et al. 2016; Rose et al. 2018; Vaughan et al. 2017).

Predicting the future hydroclimate of northwestern France is particularly challenging (Bisselink et al., 2020). While climate projections predict with a high degree of confidence that mean annual temperatures will continue to increase until the end of the 21st century in all RCP scenarios (+1.0 °C in RCP2.6, +2.2 °C in RCP4.5 and +4.5 °C in RCP8.5), projections are more uncertain for precipitation and hydrological regimes (Soubeyroux et al., 2021). This uncertainty stems from France's location, between northern Europe where annual precipitation is expected to increase, and southern Europe where it is expected to decrease (Bisselink et al., 2020). Regional climate models predict an increase in precipitation seasonality, with winter precipitation increasing by more than 10 % in nearly all RCP scenarios, and summer precipitation decreasing by -10 % to -20 % in RCP4.5 and RCP8.5 (Soubeyroux et al., 2021). In all RCP scenarios, annual cumulative discharges are expected to decrease due to increasing evapotranspiration, and discharge seasonality is expected to increase (Dayon et al., 2018). Extreme rainfall events, defined by Soubeyroux et al. (2021) as the 99th percentile of daily rainfall each year, also increase in all RCP scenarios by 10 % but with high variability among regional climate models.

The present study focused on extreme events in terms of their concentration in P and nitrate. We hypothesized that these extreme

concentration events represent particular hydroclimatic conditions such as heavy rainfall interspersed with drought, i.e., the type of events that climate scenarios predict to become more frequent in the future. To test this hypothesis, we identified events with extreme concentrations using Extreme Value Theory (EVT), and compared their concentration-discharge dynamics and hydroclimatic characteristics to those of events with non-extreme concentrations.

## 2. Materials and methods

### 2.1. Study site

The Kervidy-Naizin catchment is a 5 km<sup>2</sup> agricultural catchment located in the Brittany region, north-western France (48°00' N, 2°49' W) (Fig. 1). It belongs to the AgrHys Environmental Research Observatory, set up in 1999 to monitor long-term effects of changes in agriculture and climate on water quality (Fovet et al., 2018b). Kervidy-Naizin is also one of the French Critical Zone Observatories (OZCAR, Gaillardet et al. 2018). The catchment is drained by an intermittent stream of second Strahler order, with a drying phase that usually spans from August-October. The climate is temperate oceanic, with annual cumulative precipitation and specific discharge averaging 810 ± 180 mm and 296 ± 150 mm, respectively, from 2002 to 2017. Mean annual temperature was 11.2 ± 0.6 °C, and mean daily temperature was below 0 °C an average of 11 days per year. The topography is relatively flat, with slopes less than 5 % and an elevation of 98–140 m above sea level. The bedrock consists of impervious, locally fractured Brioverian schists capped by 1–30 m of unconsolidated weathered material and loamy soils. Previous studies have shown that the hydrology is controlled by a shallow water table whose dynamics vary seasonally and spatially depending on the distance to the stream. In the upslope part of the catchment, the water table remains below the surface throughout the year, varying in depth from 1 m to more than 8 m. The water table is shallower near the stream, generally reaching the surface from November to April/May each year and forming hydromorphic soil in 16 % of the catchment. Agriculture is the dominant land use, with confined animal production (i.e., dairy cows, pigs and poultry) being the most common. The main crop rotations are maize-winter cereals and maize-grasslands. Land cover consists of ca. 30 % winter cereals, 30 % maize and 30 % grassland, with the remaining 10 % consisting of woodland, roads, gardens and farm buildings. Mean annual nutrient inputs are 212 kgN ha<sup>-1</sup> and 62 kgP ha<sup>-1</sup>. Organic fertilizer (mainly pig slurry and cow manure) is applied from February to May, as fertilization is prohibited from July to January (March for maize). No point sources of N or P have been observed in the catchment.

### 2.2. Hydrologic and chemical monitoring

Stream water level was recorded at the outlet of the catchment every minute using a float-operated sensor (OTT Thalimedes) upstream of a rectangular weir, and then converted to discharge using a rating curve (Fovet et al., 2018b). The weather station (Cimel Enerco 516i) was located 1.1 km from the catchment outlet and recorded rainfall and temperature every hour.

We monitored total P (TP) using a high-frequency bankside analyser (Hach-Lange Sigmatax-Phosphax). See Jordan et al. (2007) for a detailed description of the Sigmatax (sample homogenization) and Phosphax (sample digestion and colorimetry measurement). Briefly, the bankside analyser measures TP concentration every 30 min via acid digestion and colorimetry using the molybdate-antimony method (DIN EN ISO 6878). TP concentration is measured using unfiltered samples and ranges from 0.01 to 5.00 mgP L<sup>-1</sup>. The Phosphax performs a daily auto-calibration using a 2 mgP L<sup>-1</sup> standard, and we performed additional controls by comparing its results to daily-to-weekly grab samples analysed in the laboratory using the same method (DIN EN ISO 6878). We monitored nitrate (NO<sub>3</sub><sup>-</sup>) in situ by measuring UV-visible absorbance

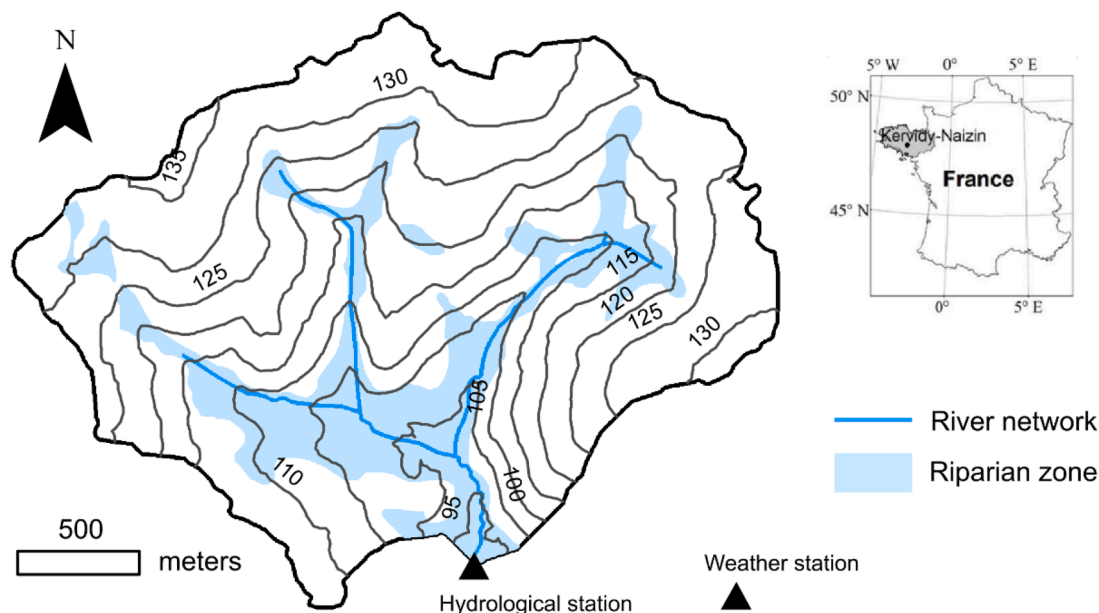


Fig. 1. Map of the Kervidy-Naizin catchment.

with a spectro::lyser™ V2 equipped with a ruck::sack autobrush from the S::CAN Company (Vienna, Austria). Nitrate concentrations are estimated from absorbance measurements every 2.5 nm from 200 to 740 nm after automatic turbidity compensation by the manufacturer's algorithm. Measurement frequency ranged from 10 to 15 min depending on the year. We then recalibrated these concentrations using a linear model fit to the daily-to-weekly grab samples analysed in the laboratory by ion chromatograph DIONEX DX 100.

Data on stream discharge, TP and nitrate were available during 2000–2023, 2016–2023 and 2011–2023, respectively. Because data resolution varied from 1 to 30 min among the parameters and years, we resampled all of the data at a 30 min resolution for the study period 2016–2023, during which 29 % and 31 % of high-frequency TP and nitrate data, respectively, were missing. Comparing the high-frequency measurements of TP and nitrate to laboratory measurements (534 and 2561 samples, respectively) revealed correlation coefficients of 0.87 and 0.97, respectively, and root mean square errors (RMSE) of  $0.02 \text{ mgP L}^{-1}$  and  $0.45 \text{ mgN L}^{-1}$  (Faucheu et al., 2024a, 2024b).

### 2.3. Data analysis

After identifying storm events from the discharge data, we analysed i) the variability in nutrient fluxes across water years and storm events; ii) nutrient concentration dynamics during storm events and their controlling factors; iii) nutrient concentrations during extreme events and their hydroclimatic properties.

#### 2.3.1. Identification of storm events

We identified storm events from the 30-min-resolution discharge data using the method of Dupas et al. (2016) and Musolff et al. (2021). The method's algorithm considers that events start when a  $5 \text{ L s}^{-1}$  increase in discharge is observed in 30 min, and that they end when discharge decreases less than  $1 \text{ L s}^{-1}$ . When storm events had multiple discharge peaks, we merged them into one event if discharge decreased less than 50 % between peaks. For this application of the algorithm, we selected only events whose discharge peak exceeded  $50 \text{ L s}^{-1}$  because visual inspection of the data showed no to only minor changes in TP and nitrate concentrations during smaller events.

#### 2.3.2. Multivariate analysis of concentration and flux dynamics

We calculated annual nutrient fluxes by multiplying the mean flow-weighted concentration by annual discharge for each water year (i.e., 1 October to 30 September). We calculated the percentage of annual flow and TP and nitrate fluxes during storm events based on instantaneous fluxes estimated during storm events and during the entire study period. No gap-filling method was used, and the estimates were based on the data available (i.e., 71 % and 69 % of the study period for TP and nitrate, respectively). We quantified variability in concentrations and fluxes variability using the coefficient of variation (CV) (i.e., mean divided by the standard deviation).

For each storm event, we calculated two descriptors of concentration dynamics and three descriptors of hydroclimatic conditions. The former were the flow-weighted concentration and a hysteresis index (HI) (Lloyd et al., 2016a). The HI was based on normalized values of concentration  $C_{i, \text{norm}}$  and discharge  $Q_{i, \text{norm}}$ , to facilitate comparison among events and between TP and nitrate:

$$C_{i, \text{norm}} = \frac{C_i - C_{\min}}{C_{\max} - C_{\min}}$$

$$Q_{i, \text{norm}} = \frac{Q_i - Q_{\min}}{Q_{\max} - Q_{\min}}$$

where  $C_i$  and  $Q_i$  are concentration and discharge at time interval  $i$ ,  $C_{\max}$  and  $C_{\min}$  are concentration maxima and minima, and  $Q_{\max}$  and  $Q_{\min}$  are discharge maxima and minima of each event.

We calculated the HI at each discharge interval as follows:

$$HI = \text{mean} (C_{i, \text{norm rising}} - C_{i, \text{norm falling}})$$

where  $C_{i, \text{norm rising}}$  and  $C_{i, \text{norm falling}}$  are  $C_{i, \text{norm}}$  in the rising and falling limbs for similar discharge values (i.e., < 5 % difference). HI ranges from  $-1$  to  $1$  with values less than  $-0.1$  indicating anticlockwise hysteresis, those greater than  $0.1$  indicating clockwise hysteresis, and those in between indicate no hysteresis or complex patterns.

To characterize the events' hydroclimatic conditions, we calculated the mean 30-day antecedent discharge ( $Q_{30d}$ , in  $\text{L s}^{-1}$ ), maximum hourly rainfall intensity ( $R_{\max}$ , in  $\text{mm h}^{-1}$ ) and mean discharge ( $Q_{\text{mean}}$ , in  $\text{L s}^{-1}$ ) during each event. The variable  $Q_{30d}$  is a proxy of a catchment's seasonal variation in wetness, which closely follows

variations in groundwater depth (Fig. SI 1). Statistical analysis of the data included multiple linear regressions (MLRs) and Mann-Whitney  $U$  tests for non-parametric comparison of two groups of variables that are not normally distributed. The MLR predicted flow-weighted mean concentrations for each storm event as a function of the three hydroclimatic variables. The MLR was used to identify hydroclimatic controls on nutrient concentrations during average storm events, to be able to compare them to those of the extreme events identified. We used only these three hydroclimatic variables in the MLR because previous studies of the same catchment during overlapping periods showed that these variables were strongly correlated with other indicators that could have been included (e.g., [Fovet et al., 2018a](#)). In addition, the three variables were proxies of the three storm characteristics that we identified in the study's hypotheses that could be influenced by climate change. We used the Bayesian Information Criterion (BIC) to select the best predictive model with one to a maximum of three predictive variables ([Schwarz, 1978](#)). Because TP concentrations were highly skewed, we log-transformed the TP data in the MLR to obtain a normal distribution; this was not necessary for nitrate.

### 2.3.3. Identification of extreme events and analysis of their hydroclimatic controls

We applied EVT as a statistical approach to identify storm events with atypical flow-weighted concentrations. We selected Generalized Pareto Distributions (GPDs) as probability distribution functions to fit values that lay over or under a certain threshold ([Embrechts et al., 1996](#)). Because TP concentration increases during storm events, while nitrate concentration decreases ([Fig. 2](#)), we applied EVT to estimate a

maximum threshold above which or minimum threshold below which, respectively, flow-weighted mean concentrations could be considered extreme.

Threshold values were estimated by testing several maximum (85th, 90th and 95th) and minimum (5th, 10th and 15th) extreme percentiles, using statistical tests and error measurements to select an adequate threshold. Specifically, we performed Komogorov-Smirnov (K-S), Mann-Whitney (M-W) and Wald-Wolfowitz (W-W) tests on the extracted extreme values to assess their conformity with GPDs, stationarity and independence, respectively (three null hypotheses  $H_0$ ). For all statistical tests, we rejected  $H_0$  at  $p < 0.05$ . In addition, the difference between the extracted extreme values and the fitted GPD was measured using the RMSE.

Characterization of the hydroclimatic conditions that control the occurrence of these extreme concentration values involved the same variables as in the multivariate analysis and we also used Mann-Whitney  $U$  test to compare extreme and non-extreme events.

We used the “extremefit” package of R to apply EVT ([Durrieu et al., 2018](#)). We used the “ggplot” package to create graphs and added predictions of Generalized Additive Models (GAM) to them to highlight patterns.

## 3. Results

### 3.1. Variability in annual and storm-event nutrient fluxes

During the study period's eight water years, annual cumulative discharge ranged from 85 mm in 2016–2017 to 613 mm in 2019–2020.

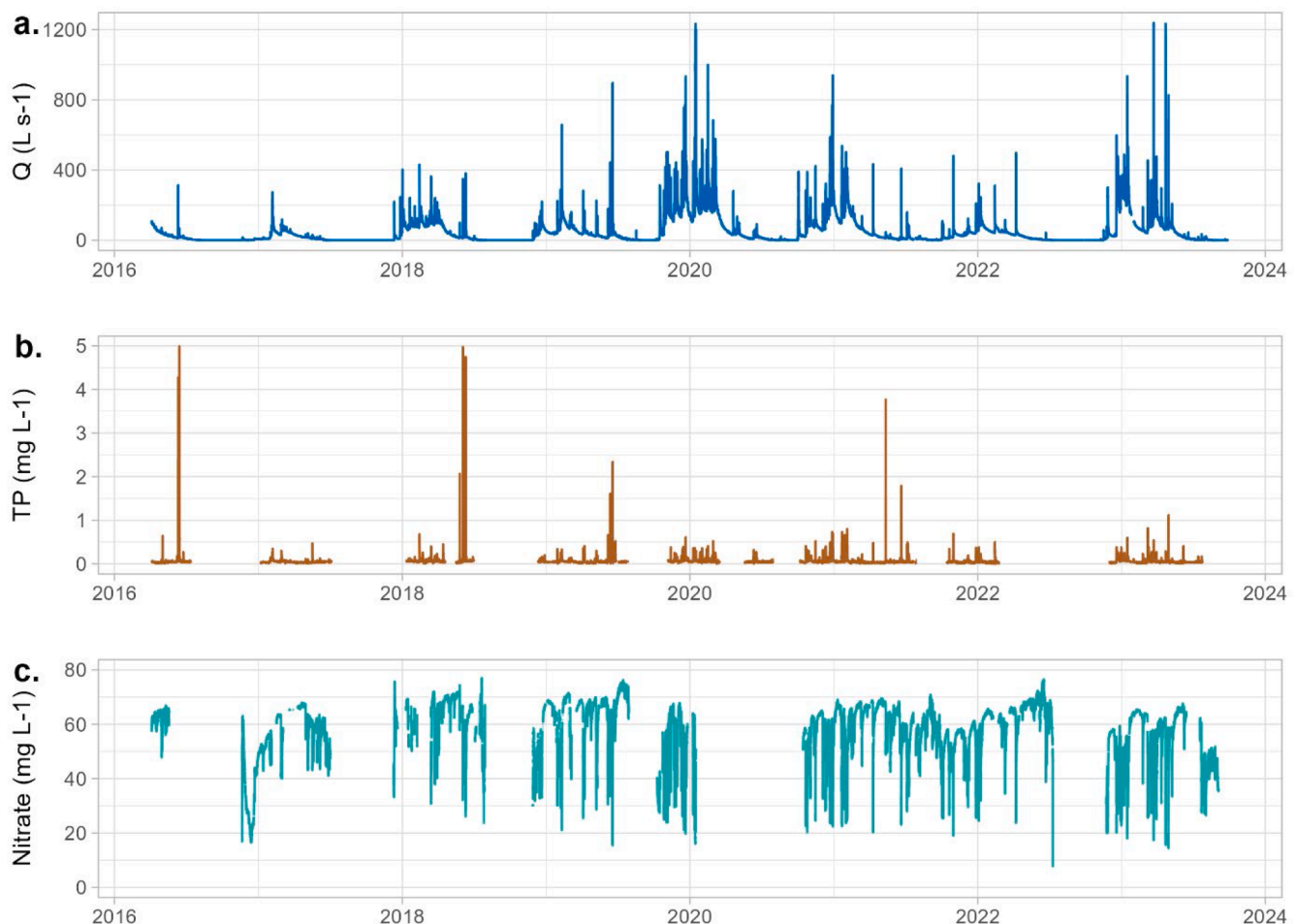


**Fig. 2.** High-frequency discharge (Q) and nitrate and total phosphorus (TP) concentrations observed from 2016 to 2023.

The stream went dry every summer, except in 2021, and the dry period lasted from 22 days in 2020 to 172 days in 2017. Annual TP fluxes ranged from 0.05 to 0.59 kgP ha<sup>-1</sup> yr<sup>-1</sup>, while annual nitrate fluxes ranged from 11 to 65 kgN ha<sup>-1</sup> yr<sup>-1</sup>, and both were strongly correlated with annual cumulative discharge ( $\rho = 0.98$  for both). Overall, 200 storm events were detected, of which 155 had been monitored for TP and 142 for nitrate. Missing data due to instrument breakdowns happened randomly, while missing data due to late restart of the instrument after the summer dry period led us to miss the first event of the hydrological year almost systematically. These 200 events represented 5 % of the period's duration and 25 % of its total discharge. TP fluxes during storm events represented 53 % of total annual flux, while nitrate fluxes during storm events represented only 19 % of total annual flux.

The variability in instantaneous discharge (CV = 133 %) was similar to that in TP concentrations (CV = 135 %), both of which were greater than that in nitrate concentrations (CV = 18 %). Across all storm events, the variability in mean discharge (CV = 53 %) was lower than that in flow-weighted mean TP concentrations (CV = 125 %) but higher than that in flow-weighted mean nitrate concentrations (CV = 16 %). Accordingly, across all events, the variability in mean TP fluxes (CV = 87 %) was higher than that in mean nitrate fluxes (CV = 48 %).

Relationships between mean event fluxes and mean event discharges showed positive trends for TP and nitrate, suggesting an overall transport limitation (Fig. 3). As mean event discharge increased, the slope of the GAM smoothed lines increased for TP and decreased for nitrate, suggesting increasing source availability for TP during high flows and some degree of source limitation for nitrate. These flux-discharge relationships showed several outliers, especially for TP. During these events, which were triggered by high rainfall intensity, TP fluxes were up to nine times larger than the GAM prediction (Fig. 3a). Conversely, for nitrate, fluxes during events triggered by high rainfall intensity were smaller than the GAM prediction (Fig. 3b). EVT aims to identify these events and specify the hydroclimatic conditions in which they occurred (Section 3.3.).

### 3.2. Controls on nutrient dynamics

Mean flow-weighted TP concentrations during storm events tended to increase as event discharge increased and antecedent discharge

decreased, while mean flow-weighted nitrate concentrations tended to decrease (Fig. 4). Mean event flow-weighted TP concentrations tended to increase as rainfall intensity increased, flow-weighted nitrate concentrations tended to decrease (Fig. SI 2).

The best MLR model to predict flow-weighted concentrations, based on minimization of the BIC, included all three explanatory variables (i. e., Q30d, Qmean, Rmax) and explained 62 % and 53 % of the variance in flow-weighted concentrations across events for TP and nitrate, respectively:

$$\log(\text{TP}) = -2.49 - 0.0039 * \text{Q30d} + 0.0032 * \text{Qmean} + 0.12 * \text{Rmax}$$

$$\text{Nitrate} = 47.5 + 0.061 * \text{Q30d} - 0.059 * \text{Qmean} - 0.49 * \text{Rmax}$$

TP-discharge relationships had a similar number of clockwise and anticlockwise loops (41 and 45, respectively) and even more events with no clear hysteresis pattern (69 occurrences). Nitrate-discharge relationships had more clockwise than anticlockwise loops (65 and 23, respectively), and 54 events with no clear hysteresis pattern. For TP, events with a clockwise hysteresis were associated with higher event discharge, antecedent discharge and rainfall intensities, than anticlockwise events (Fig. 5). For nitrate, events with a clockwise hysteresis were associated with higher antecedent discharge and lower rainfall intensity than anticlockwise events. Clockwise and anticlockwise nitrate-discharge loops did not differ in mean event discharge. Hydroclimatic conditions for events with no hysteresis loop tended to lie between those with clockwise and anticlockwise hystereses, for both nutrients (Fig. 5).

### 3.3. Extreme concentrations during storm events and their hydrological controls

When applying EVT to the flow-weighted mean TP and nitrate concentrations, we identified 10 and 14 extreme events for TP and nitrate, respectively, considering the 90th percentile as the maximum threshold for TP and the 10th percentile as the minimum threshold for nitrate (Table SI 1). We identified three events as extreme for both TP and nitrate. The supplementary Fig. SI 3 confirms that these extreme events corresponded to the outliers observed previously (Fig. 3). During extreme TP events, flow-weighted mean concentrations were 200 %–

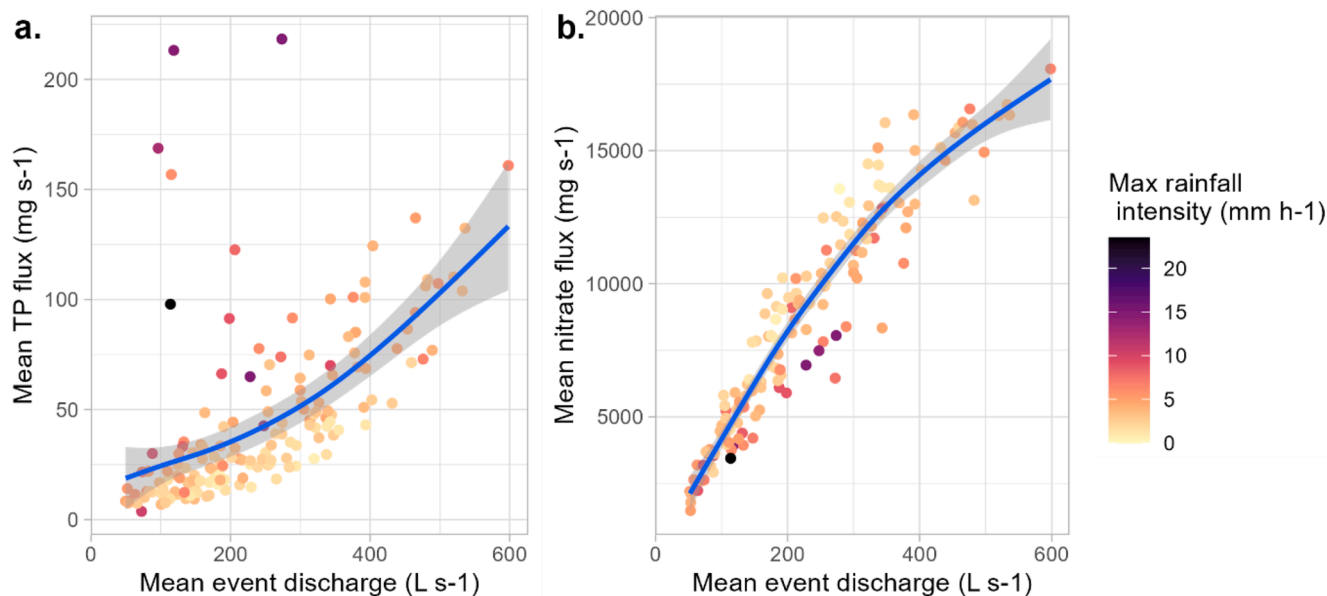
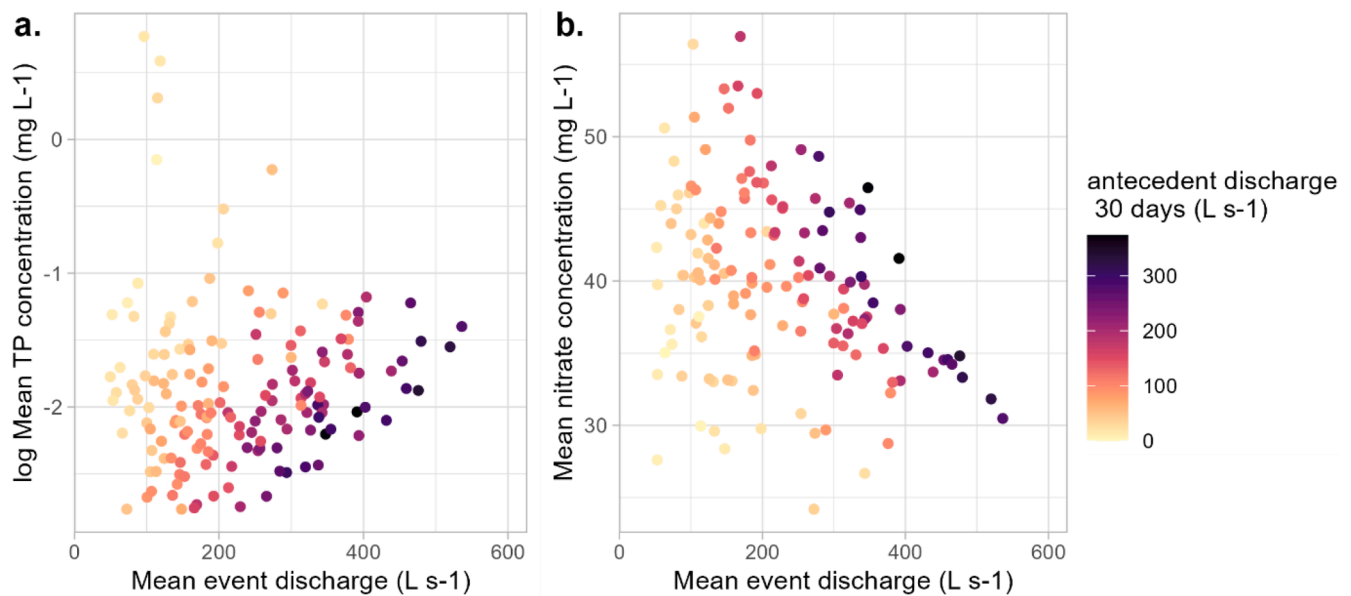


Fig. 3. Relationships between mean event fluxes and mean event discharges for (a) total phosphorus (TP) and (b) nitrate. Each dot represents a storm event, and its colour represents the event's maximum hourly rainfall intensity. The blue smoothing line is a generalized additive model (GAM) and the grey band a 95 % confidence interval.



**Fig. 4.** Relationships between flow-weighted mean event concentrations and mean event discharge for (a) total phosphorus (TP) and (b) nitrate. Each dot represents a storm event and its colour represents the event's antecedent discharge.

1400 % higher than the average of non-extreme events. During extreme nitrate events, flow-weighted mean concentrations were 21 %–41 % lower than the average of non-extreme events.

These extreme flow-weighted mean concentrations of both TP and nitrate corresponded to high rainfall intensity and low antecedent discharge, but no particular conditions of mean event discharge (Fig. 6). Extreme TP events had a HI close to 0, indicating weak hysteresis loops, while extreme nitrate events had lower HI, indicating more anticlockwise loops than those of average events. These extreme events tended to occur in the spring for TP and autumn for nitrate (i.e., at the end or beginning of the hydrological year, respectively).

## 4. Discussion

### 4.1. Controls on nutrient fluxes and concentrations in average conditions

Annual nutrient fluxes were strongly correlated with annual cumulative discharge, which is typical for transport-limited systems. Transport limitation is the most common pattern in intensively farmed catchments, where nutrient inputs are high and their source availability never limits annual exports (Basu et al., 2010; Mellander et al., 2014; Molenat et al., 2008; Musolff et al., 2015). In the Kervidy-Naizin catchment, the CV of instantaneous discharge exceeded that of nitrate concentration, but was similar to that of TP concentration. Nitrate is thus chemostatic, while TP is more chemodynamic. Chemostatic export regimes associated with a dilution signal during runoff events is typical for pollutants that accumulate in groundwater, while chemodynamic export regimes associated with an accretion signal during events is more typical for pollutants that lie near the soil surface (Ebeling et al., 2021; Knapp et al., 2022; Stewart et al., 2022; Zhi et al., 2019).

Storm events are the main drivers of intra-annual variability in nutrient concentrations in small catchments such as Kervidy-Naizin (Fig. 2), unlike larger catchments, where marked seasonal variations are apparent in concentration time series (Abbott et al., 2018; Casquin et al., 2020; Guillemot et al., 2021). In Kervidy-Naizin, storm events represented the majority of TP flux, while the percentage of nitrate flux that occurred during events was lower than that of cumulative discharge. This is consistent with the observed accretion pattern for TP and dilution pattern for nitrate during events. A previous study of P fluxes in the Kervidy-Naizin used low-frequency TP and soluble reactive P (SRP) data

from 2007 to 2013 to calibrate an empirical model, which showed that TP annual fluxes ranged from 0.18 to 0.63 kgP ha<sup>-1</sup> yr<sup>-1</sup> of which 24 % was SRP (Minaudo et al., 2017). The flux estimates of the present study were similar, but we could not assess the percentage of SRP because the Phosphax analyser has no filtration system. As for inter-annual nutrient fluxes, most fluxes across events were transport-limited, although the largest storm events indicated an increase in TP source availability and some degree of source limitation for nitrate. These deviations from a purely transport-driven system seem due to large contributions during high-discharge events of overland flow, which has high TP and low nitrate concentrations (Fovet et al., 2018a; Speir et al., 2023).

During storm events, we observed the three types of hysteresis loops – clockwise, anticlockwise and no hysteresis – for both nutrients. Previous studies of Kervidy-Naizin and other catchments found that particulate P had clockwise hystereses while soluble P had anticlockwise hystereses (Dupas et al., 2015). Hence, the loop direction of TP hysteresis can depend on the proportions of particulate and soluble forms. Hystereses turn clockwise when a proximal source is mobilized (i.e., stream bed sediment and bank erosion) or during events with infiltration-excess overland flow and erosion. These kinds of events export mainly particulate P forms and occur when discharge is high or when intensive rain falls after a dry period, as confirmed by the analysis of hydrological conditions (Section 3.2.). Conversely, hysteresis turn anticlockwise when a more distal source is mobilized, such as when groundwater rises in the riparian zone during the event and causes subsurface flow or saturation-excess runoff, which usually export more soluble P forms (Gu et al., 2023). Nitrate-discharge relationships for most events had no hysteresis or clockwise hysteresis, indicating a dilution signal or the contribution of denitrified riparian water in the falling limb of the hydrograph (Fovet et al., 2018a; Lloyd et al., 2016b; Musolff et al., 2021; Rose et al., 2018). Nitrate-discharge relationships can form anticlockwise hystereses when concentrations are low in the rising limb of the hydrograph or high in the falling limb. Nitrate concentrations in the rising limb can be low when overland flows bring large amounts of rainwater, which is consistent with our observation of high rainfall intensities for anticlockwise nitrate hystereses. Nitrate concentrations in the falling limb can be high when riparian soils are well aerated, which promotes N mineralization and limits denitrification. These conditions are consistent with the low antecedent discharge - associated with low groundwater level in the riparian zone (Fovet et al.,

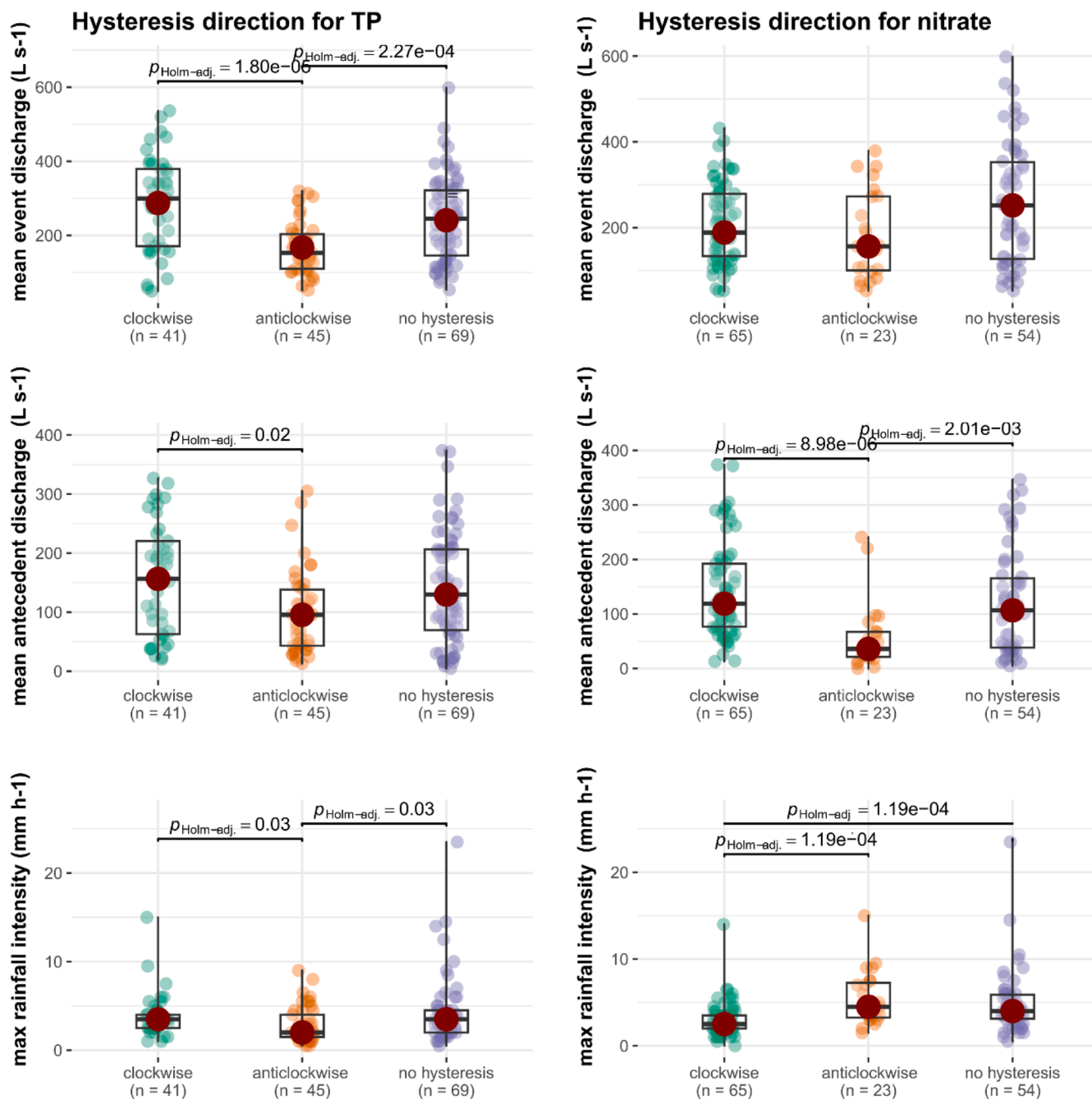


Fig. 5. Comparison of hydrological conditions as a function of direction of the concentration-discharge hysteresis for total phosphorus (TP) and nitrate. The p-values are derived from Mann-Whitney U tests.

2018a) – that we observed for anticlockwise nitrate hysteresses.

4.2. Controls on nutrient fluxes and concentrations during extreme events

EVT identified 10 extreme events out of 155 for TP, and 14 extreme events out of 142 for nitrate. These events corresponded to extreme accretion patterns for TP and extreme dilution patterns for nitrate. Flow-weighted concentrations during extreme events differed from those of average events more for TP (i.e., up to 14 times as high) than for nitrate (i.e., up to 41 % lower) because the catchment has large P sources, such as over fertilized fields and fields sensitive to erosion, that are rarely connected to the stream except during extreme events (Cassidy et al., 2019; Matos-Moreira et al., 2015). In intensively farmed catchments

such as Kervidy-Naizin, recent inorganic or organic fertilizer inputs, and degradation of soil aggregate stability after seedbed preparation for spring crops may exacerbate erosion of P-rich soil particles in the spring (Le Bissonnais et al., 2002). In addition to incidental losses of recently applied fertilizers, temperature and drought dependent P mobilization mechanisms such as cell lysis may play a role in the spring and summer time (Turner and Haygarth, 2001). For nitrate, no end-member can be less concentrated than rainfall, which contains virtually no nitrate and already contributes during non-extreme events.

The extreme events identified for both nutrients occurred when antecedent discharge was low and rainfall intensity was high. Antecedent discharge can be as low as zero in the Kervidy-Naizin catchment when a storm event occurs after the summer drought. Rainfall intensity



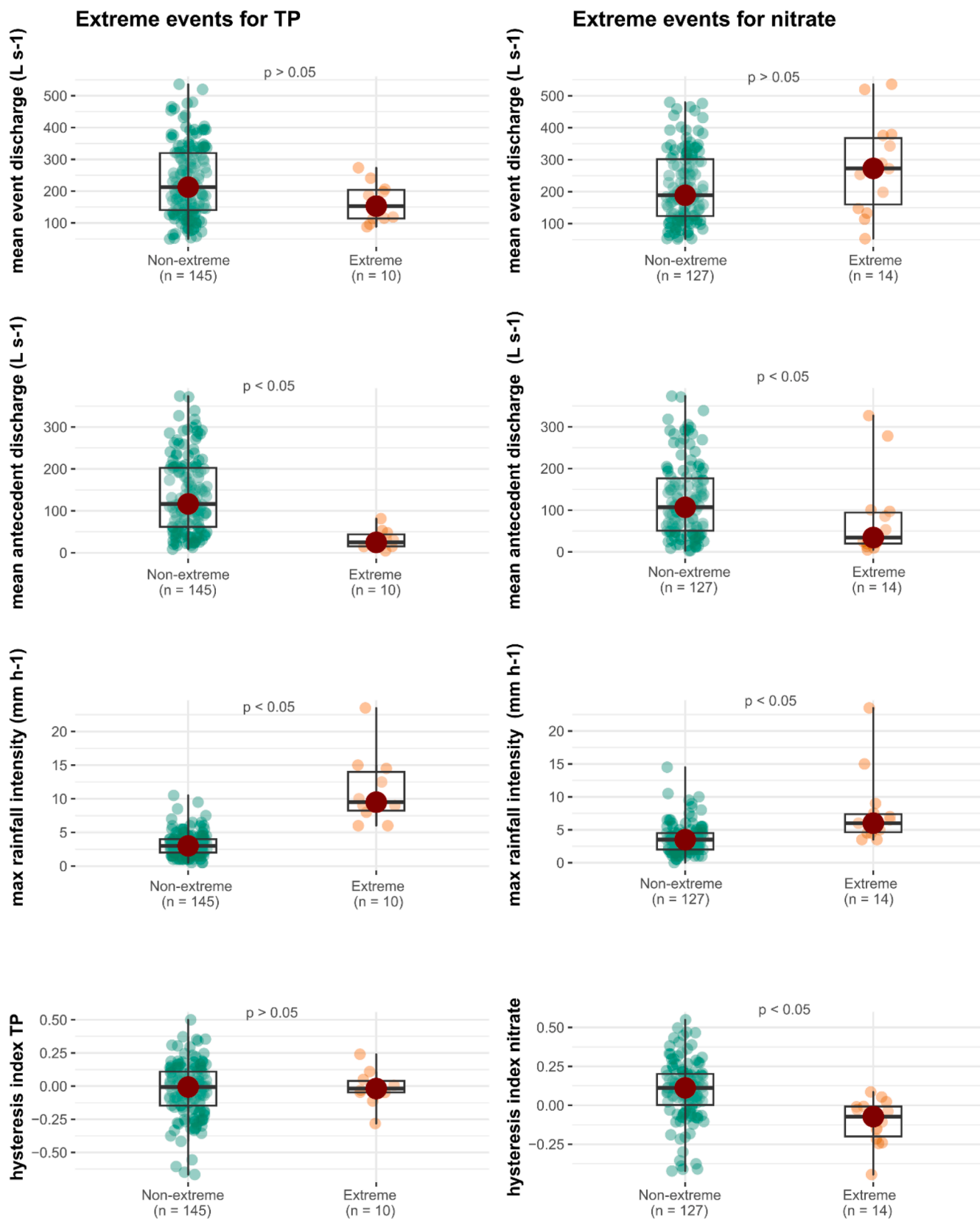


Fig. 6. Comparison of hydrological conditions for extreme events versus non-extreme events for flow-weighted mean concentrations of total phosphorus (TP) and nitrate. The p-values are derived from Mann-Whitney *U* tests.

reached 23 mm/h during one extreme events (i.e., seven times as high as that of average events of 2016–2023). According to climate projections, such extreme hydroclimatic conditions may become more frequent in the future (Soubeyrou et al., 2021). The dry intermittent phase that the Kervidy Naizin catchment already experiences is also likely to become longer under future climate conditions, which may exacerbate the nutrient export pattern observed during the extreme events observed in the present study. Hence, these extreme TP concentration peaks and nitrate dilution episodes are likely to occur more frequently in the future in this catchment, as well as in other catchments that have a similar climate, soil and land use.

Extreme flow-weighted mean concentrations do not, however, result in extreme nutrient fluxes, as also observed in catchments of the United Kingdom (Ockenden et al., 2016), because these extreme concentrations were not associated with particularly high discharges (Fig. 6), and several events not classified as extreme had larger fluxes (Fig. SI 3). Nonetheless, they occurred mainly in the autumn and spring, when discharge was relatively low. The modest fluxes of highly concentrated TP and highly diluted nitrate during these events could therefore be large for the season. Finally, N:P ratios during extreme events were particularly low (Fig. SI 4) due to the exceptionally high TP and low nitrate concentrations, which may have major ecological impacts (Wachholz et al., 2023).

#### 4.3. Implications for the future of nutrient fluxes and concentration in a context of climate change

This study found that extreme TP concentration peaks and nitrate dilution episodes occurred during storm events with high rainfall intensities after periods of low flow or drought. According to the most recent hydroclimatic projections for France (Dayon et al., 2018; Soubeyrou et al., 2021) and elsewhere in Europe (Eisner et al., 2017; van Vliet et al., 2013), this type of hydroclimatic events will occur more frequently in the future. Extrapolation from past observations would therefore suggest higher frequency and amplitudes of extreme TP concentration peaks and nitrate dilution episodes in the future.

However, the increasing frequency and intensity of droughts and storms is only one aspect only of climate change, whose many aspects will interact and shape our future hydroclimate (Mellander et al., 2018; Mellander and Jordan, 2021). For example, it is difficult to predict the effects of increasing temperatures and evapotranspiration, which will play large roles in the future (Van Vliet et al., 2023; Li et al., 2024). In the short term, P and N export will likely continue to be transport-limited on an annual basis, as agricultural catchments contain large legacy nutrient sources; consequently, annual nutrient fluxes should remain proportional to annual cumulative discharge (Dupas et al., 2017; Molenat et al., 2008) and thus decrease as annual discharge decreases (Dayon et al., 2018). Short-term observations of storm responses capture only the delivery signal of nutrient export from catchment legacy sources to streams (Haygarth et al., 2005). In the medium term, climate change will also influence the formation of these legacy sources through its influence on nutrient mobilization mechanisms such as P solubilisation and nitrate leaching (Forber et al., 2018; Gu et al., 2023; Ockenden et al., 2017).

Finally, agricultural catchments are socio-ecosystems that respond to global changes, such as by changing farming systems and practices. Previous studies has illustrated how the study region's farming systems changed its nitrogen surpluses, which nearly tripled from 1976 to 2000 and decreased significantly from 2000 to 2015 (Dupas et al., 2020). Predicting future nutrient fluxes and concentrations in agricultural streams requires carefully examining of socio-economic scenarios (Ockenden et al., 2017), which for the study region could follow pathways that differ greatly in characteristics such as the main production systems, degree of desintensification and use of irrigation (Bretagne, 2023).

## 5. Conclusion

Climate change projections indicate that hydroclimatic extremes (i.e., floods and droughts) will increase in frequency and intensity in the temperate zone. We analysed high-frequency nutrient-monitoring data from eight water years and identified extreme events in terms of P concentration peaks and nitrate concentration minima. These extreme events occur during episodes of extreme rainfall intensity during periods of low-flow or drought, which are projected to become more frequent in the future. During these extreme events, infiltration-excess overland flow exports large amounts of P and dilutes the nitrate contributed by groundwater, while groundwater fluctuation in the riparian zone and streambed remobilization control nutrient export during non-extreme events. This retrospective analysis provides insights into future nutrient dynamics in streams that drain agricultural catchments. Future assessments should include other aspects of climate change such as temperature increases, and the changes in agricultural practices induced by global change. Integrated catchment models should be evaluated for their ability to simulate extreme events before being used to simulate of future climatic and agricultural scenarios.

### CRediT authorship contribution statement

**Rémi Dupas:** Writing – review & editing, Writing – original draft, Project administration, Methodology, Investigation, Formal analysis, Data curation, Conceptualization. **Mikaël Faucheux:** Project administration, Investigation, Formal analysis, Data curation. **Tristan Senga Kiessé:** Writing – original draft, Investigation, Formal analysis. **Andrés Casanova:** Formal analysis, Data curation, Conceptualization. **Nicolai Brekenfeld:** Writing – review & editing, Investigation, Conceptualization. **Ophélie Fovet:** Writing – review & editing, Project administration, Investigation, Conceptualization.

### Declaration of competing interest

The authors declare that they have no known competing financial interests or personal relationships that could have appeared to influence the work reported in this paper.

### Data availability

Data available <https://entrepot.recherche.data.gouv.fr/dataverse/agrhys>.

### Supplementary materials

Supplementary material associated with this article can be found, in the online version, at [doi:10.1016/j.watres.2024.122108](https://doi.org/10.1016/j.watres.2024.122108).

## References

- Abbott, B.W., Moatar, F., Gauthier, O., Fovet, O., Antoine, V., Ragueneau, O., 2018. Trends and seasonality of river nutrients in agricultural catchments: 18 years of weekly citizen science in France. *Sci. Total Environ.* 624, 845–858.
- Abily, M., Vicenç, A., Gernjak, W., Rodríguez-Roda, I., Poch, M., Corominas, L., 2021. Climate change impact on EU rivers' dilution capacity and ecological status. *Water* 199, 117166.
- Aubert, A.H., Tavenard, R., Emonet, R., de Lavenne, A., Malinowski, S., Guyet, T., et al., 2013. Clustering flood events from water quality time series using Latent Dirichlet Allocation model. *Water. Resour. Res.* 49, 8187–8199.
- Basu, N.B., Destouni, G., Jawitz, J.W., Thompson, S.E., Loukinova, N.V., Darracq, A., et al., 2010. Nutrient loads exported from managed catchments reveal emergent biogeochemical stationarity. *Geophys. Res. Lett.* 37, 23404.
- Bieroza, M., Acharya, S., Benisch, J., ter Borg, R.N., Hallberg, L., Negri, C., et al., 2023. Advances in catchment science, hydrochemistry, and aquatic ecology enabled by high-frequency water quality measurements. *Environ. Sci. Technol.* 57, 4701–4719.
- Bieroza, M.Z., Heathwaite, A.L., 2015. Seasonal variation in phosphorus concentration-discharge hysteresis inferred from high-frequency in situ monitoring. *J. Hydrol.* 524, 333–347.

- Bisselink, B., Bernhard, J., Gelati, E., Adamovic, M., Guenther, S., Mentaschi, L., et al., 2020. Climate Change and Europe's Water Resources. Publications Office of the European Union, Luxembourg. EUR 29951.
- Bol, R., Gruau, G., Mellander, P.E., Dupas, R., Bechmann, M., Skarbovik, E., et al., 2018. Challenges of reducing phosphorus based water eutrophication in the agricultural landscapes of Northwest Europe. *Front. Mar. Sci.* 5, 276.
- Bretagne Cdad. *Agricultures bretonnes 2040, cinq scenarios d'avenir*. 2023.
- Casquin, A., Gu, S., Dupas, R., Petitjean, P., Gruau, G., Durand, P., 2020. River network alteration of C-N-P dynamics in a mesoscale agricultural catchment. *Sci. Total Environ.* 749, 141551.
- Cassidy, R., Thomas, I.A., Higgins, A., Bailey, J.S., Jordan, P., 2019. A carrying capacity framework for soil phosphorus and hydrological sensitivity from farm to catchment scales. *Sci. Total Environ.* 687, 277–286.
- Dayon, G., Boé, J., Martin, É., Gailhard, J., 2018. Impacts of climate change on the hydrological cycle over France and associated uncertainties. *Comptes Rendus Geosci.* 350, 141–153.
- Dupas, R., Ehrhardt, S., Musolf, A., Fovet, O., Durand, P., 2020. Long-term nitrogen retention and transit time distribution in agricultural catchments in western France. *Environ. Res. Lett.* 15, 115011.
- Dupas, R., Gascuel-Odoux, C., Gilliet, N., Grimaldi, C., Gruau, G., 2015. Distinct export dynamics for dissolved and particulate phosphorus reveal independent transport mechanisms in an arable headwater catchment. *Hydrol. Process.* 29, 3162–3178.
- Dupas, R., Jomaa, S., Musolf, A., Borchardt, D., Rode, M., 2016. Disentangling the influence of hydroclimatic patterns and agricultural management on river nitrate dynamics from sub-hourly to decadal time scales. *Sci. Total Environ.* 571, 791–800.
- Dupas, R., Mellander, P.E., Gascuel-Odoux, C., Fovet, O., McAleer, E.B., McDonald, N., et al., 2017. The role of mobilisation and delivery processes on contrasting dissolved nitrogen and phosphorus exports in groundwater fed catchments. *Sci. Total Environ.* 1275–1287.
- Durrieu, G., Grama, I., Jaunatre, K., Pham, Q., Tricot, J., 2018. ExtremeFit: a package for extreme quantiles. *J. Stat. Softw.* 87, 1–20.
- Ebeling, P., Kumar, R., Weber, M., Knoll, L., Fleckenstein, J.H., Musolf, A., 2021. Archetypes and controls of riverine nutrient export across german catchments. *Water. Resour. Res.* 57, e2020WR028134.
- Eisner, S., Flörke, M., Chamorro, A., Daggupati, P., Donnelly, C., Huang, J., et al., 2017. An ensemble analysis of climate change impacts on streamflow seasonality across 11 large river basins. *Clim. Change* 141, 401–417.
- Embrechts, P., Klüppelberg, C., Mikosch, T., 1996. *Modelling extremal events for insurance and finance*. Stochastic Modelling and Applied Probability. Springer.
- Faucheux, M., Dupas, R., Bouillis, C., Carteaux, L., Casanova, A., Ruiz, L., et al., 2024a. High-frequency measurement of Total Phosphorus and Total Reactive Phosphorus in the Kervidy-Naizin catchment (2016-2023). *Recherche Data Gov V1*.
- Faucheux, M., Petitjean, P., Bouillis, C., Carteaux, L., Jeanneau, L., Ruiz, L., et al., 2024b. High-frequency measurement of Nitrate and Dissolved Organic Carbon in the Kervidy-Naizin catchment (2010-2023). *Recherche Data Gov V1*.
- Forber, K.J., Withers, P.J.A., Ockenden, M.C., Haygarth, P.M., 2018. The phosphorus transfer continuum: a framework for exploring effects of climate change. *Agric. Environ. Lett.* 3, 180036.
- Fovet, O., Humbert, G., Dupas, R., Gascuel-Odoux, C., Gruau, G., Jaffrezic, A., et al., 2018a. Seasonal variability of stream water quality response to storm events captured using high-frequency and multi-parameter data. *J. Hydrol.* 559, 282–293.
- Fovet, O., Ruiz, L., Gruau, G., Akkal, N., Aquilina, L., Busnot, S., et al., 2018b. AgrHyS: an observatory of response times in agro-hydro systems. *Vadose Zone J.* 17, 1–16.
- Gaillardet, J., Braud, I., Hankard, F., Anquetin, S., Bour, O., Dorfliger, N., et al., 2018. OZCAR: the French network of critical zone observatories. *Vadose Zone J.* 17, 1–24.
- Gascuel-Odoux, C., Fovet, O., Gruau, G., Ruiz, L., Merot, P., 2018. Evolution of scientific questions over 50 Years in the Kervidy-Naizin catchment: from catchment hydrology to integrated studies of biogeochemical cycles and agroecosystems in a rural landscape. *Cuadernos Investig. Geogr.* 44, 535–555.
- Gu, S., Couic, E., Gruau, G., Casquin, A., 2023. Conventional soil test phosphorus failed to accurately predict dissolved phosphorus release in agricultural hydromorphic soils in Brittany, Western France. *Geoderma Regional* 34, e00689.
- Guillemot S., Fovet O., Gascuel-Odoux C., Gruau G., Casquin A., Curie F., et al. *Spatio-temporal controls of C-N-P dynamics across headwater catchments of a temperate agricultural region from public data analysis*. HESSD 2021.
- Haygarth, P.M., Condon, L.M., Heathwaite, A.L., Turner, B.L., Harris, G.P., 2005. The phosphorus transfer continuum: linking source to impact with an interdisciplinary and multi-scaled approach. *Sci. Total Environ.* 344, 5–14.
- Hirabayashi, Y., Kanae, S., Emori, S., Oki, T., Kimoto, M., 2008. Global projections of changing risks of floods and droughts in a changing climate. *Hydrol. Sci. J.-J. Sci. Hydrol.* 53, 754–772.
- Jordan, P., Arnscheidt, A., McGrogan, H., McCormick, S., 2007. Characterising phosphorus transfers in rural catchments using a continuous bank-side analyser. *Hydrol. Earth. Syst. Sci.* 11, 372–381.
- Jin, L., Whitehead, P.G., Sarkar, S., Sinha, R., Futter, M.N., Butterfield, D., et al., 2015. Assessing the impacts of climate change and socio-economic changes on flow and phosphorus flux in the Ganga river system. *Environ. Sci.-Process. Impacts* 17, 1098–1110.
- Kincaid, D.W., Seybold, E.C., Adair, E.C., Bowden, W.B., Perdril, J.N., Vaughan, M.C.H., et al., 2020. Land use and season influence event-scale nitrate and soluble reactive phosphorus exports and export stoichiometry from headwater catchments. *Water. Resour. Res.* 56, e2020WR027361.
- Knapp, J.L.A., Li, L., Musolf, A., 2022. Hydrologic connectivity and source heterogeneity control concentration-discharge relationships. *Hydrol. Process.* 36, e14683.
- Le Bissonnais, Y., Cros-Cayot, S., Gascuel-Odoux, C., 2002. Topographic dependence of aggregate stability, overland flow and sediment transport. *Agronomie* 22, 489–501.
- Li, L., Knapp, J.L.A., Lintern, A., Ng, G.H.C., Perdril, J., Sullivan, P.L., et al., 2024. River water quality shaped by land-river connectivity in a changing climate. *Nat. Clim. Chang.* 14, 225–237.
- Lloyd, C.E.M., Freer, J.E., Johnes, P.J., Collins, A.L., 2016a. Technical note: testing an improved index for analysing storm discharge-concentration hysteresis. *Hydrol. Earth. Syst. Sci.* 20, 625–632.
- Lloyd, C.E.M., Freer, J.E., Johnes, P.J., Collins, A.L., 2016b. Using hysteresis analysis of high-resolution water quality monitoring data, including uncertainty, to infer controls on nutrient and sediment transfer in catchments. *Sci. Total Environ.* 543, 388–404.
- Matos-Moreira, M., Lemercier, B., Michot, D., Dupas, R., Gascuel-Odoux, C., 2015. Using agricultural practices information for multiscale environmental assessment of phosphorus risk. *Geophys. Res. Abs.* 17.
- Melland, A.R., Mellander, P.E., Murphy, P.N.C., Wall, D.P., Mehan, S., Shine, O., et al., 2012. Stream water quality in intensive cereal cropping catchments with regulated nutrient management. *Environ. Sci. Policy.* 24, 58–70.
- Mellander, P.-E., Jordan, P., Bechmann, M., Fovet, O., Shore, M.M., McDonald, N.T., et al., 2018. Integrated climate-chemical indicators of diffuse pollution from land to water. *Sci. Rep.* 8, 944.
- Mellander, P.E., Jordan, P., 2021. Charting a perfect storm of water quality pressures. *Sci. Total Environ.* 787, 147576.
- Mellander, P.E., Jordan, P., Shore, M., Melland, A.R., Shortle, G., 2015. Flow paths and phosphorus transfer pathways in two agricultural streams with contrasting flow controls. *Hydrol. Process.* 29, 3504–3518.
- Mellander, P.E., Melland, A.R., Murphy, P.N.C., Wall, D.P., Shortle, G., Jordan, P., 2014. Coupling of surface water and groundwater nitrate-N dynamics in two permeable agricultural catchments. *J. Agric. Sci.* 152, S107–S124.
- Minaudo, C., Dupas, R., Gascuel-Odoux, C., Fovet, O., Mellander, P.E., Jordan, P., et al., 2017. Nonlinear empirical modeling to estimate phosphorus exports using continuous records of turbidity and discharge. *Water. Resour. Res.* 53, 7499–8134.
- Molénat, J., Gascuel-Odoux, C., Ruiz, L., Gruau, G., 2008. Role of water table dynamics on stream nitrate export and concentration in agricultural headwater catchment (France). *J. Hydrol.* 348, 363–378.
- Mosley, L.M., 2015. Drought impacts on the water quality of freshwater systems; review and integration. *Earth. Sci. Rev.* 140, 203–214.
- Musolf, A., Schmidt, C., Selle, B., Fleckenstein, J.H., 2015. Catchment controls on solute export. *Adv. Water. Resour.* 86, 133–146.
- Musolf, A., Zhan, Q., Dupas, R., Minaudo, C., Fleckenstein, J.H., Rode, M., et al., 2021. Spatial and temporal variability in concentration-discharge relationships at the event scale. *Water. Resour. Res.* 57, e2020WR029442.
- Ockenden, M.C., Deasy, C.E., Benskin, C.M.H., Beven, K.J., Burke, S., Collins, A.L., et al., 2016. Changing climate and nutrient transfers: evidence from high temporal resolution concentration-flow dynamics in headwater catchments. *Sci. Total Environ.* 548, 325–339.
- Ockenden, M.C., Hollaway, M.J., Beven, K.J., Collins, A.L., Evans, R., Falloon, P.D., et al., 2017. Major agricultural changes required to mitigate phosphorus losses under climate change. *Nat. Commun.* 8, 161.
- Pörtner, H.-O., Roberts, D.C., Poloczanska, E.S., Mintenbeck, K., Tognor, M., Alegria, A., et al., 2022. *Climate Change 2022: Impacts, Adaptation and Vulnerability*. Contribution of Working Group II to the Sixth Assessment Report of the Intergovernmental Panel On Climate Change. Cambridge University Press, pp. 37–118.
- Rode, M., Wade, A.J., Cohen, M.J., Hensley, R.T., Bowes, M.J., Kirchner, J.W., et al., 2016. Sensors in the stream: the high-frequency wave of the present. *Environ. Sci. Technol.* 50, 10297–10307.
- Rose, L.A., Karwan, D.L., Godsey, S.E., 2018. Concentration-discharge relationships describe solute and sediment mobilization, reaction, and transport at event and longer timescales. *Hydrol. Process.* 32, 2829–2844.
- Schwarz, G., 1978. Estimating the dimension of a model. *Ann. Stat.* 6, 461–464, 4.
- Soubeyrou J.M., Bernus S., Corre L., Drouin A., Dubuisson B., Etchevers P., et al. *Les nouvelles projections climatiques de référence DRIAS 2020 pour la métropole*. Météo France 2021.
- Speir, S.L., Rose, L.A., Blaszczyk, J.R., Kincaid, D.W., Fazekas, H.M., Webster, A.J., et al., 2023. Catchment concentration-discharge relationships across temporal scales: a review. *WIREs Water* 11, e1702.
- Stewart, B., Shanley, J.B., Kirchner, J.W., Norris, D., Adler, T., Bristol, C., et al., 2022. Streams as mirrors: reading subsurface water chemistry from stream chemistry. *Water. Resour. Res.* 58, e2021WR029931.
- Strohmeier, L., Fovet, O., Akkal-Corfini, N., Dupas, R., Durand, P., Faucheux, M., et al., 2020. Multimtemporal relationships between the hydroclimate and exports of carbon, nitrogen, and phosphorus in a small agricultural watershed. *Water. Resour. Res.* 56, e2019WR026323.
- Turner, B.L., Haygarth, P.M., 2001. Biogeochemistry - phosphorus solubilization in rewetted soils. *Nature* 411, 258–258.
- van Vliet, M.T.H., Franssen, W.H.P., Yearsley, J.R., Ludwig, F., Haddeland, I., Lettenmaier, D.P., et al., 2013. Global river discharge and water temperature under climate change. *Glob. Environ. Change-Hum. Policy Dimens.* 23, 450–464.

- Van Vliet, M.T.H., Thorslund, J., Stokal, M., Hofstra, N., Flörke, M., Macedo, H.E., et al., 2023. Global river water quality under climate change and hydroclimatic extremes. *Nat. Rev. Earth Environ.* 4, 687–702.
- Vaughan, M.C.H., Bowden, W.B., Shanley, J.B., Vermilyea, A., Sleeper, R., Gold, A.J., et al., 2017. High-frequency dissolved organic carbon and nitrate measurements reveal differences in storm hysteresis and loading in relation to land cover and seasonality. *Water. Resour. Res.* 53, 5345–5363.
- Wachholz, A., Dehaspe, J., Ebeling, P., Kumar, R., Musolf, A., Saavedra, F., et al., 2023. Stoichiometry on the edge-humans induce strong imbalances of reactive C:N:P ratios in streams. *Environ. Res. Lett.* 18, 044016.
- Zhi, W., Li, L., Dong, W.M., Brown, W., Kaye, J., Steefel, C., et al., 2019. Distinct source water chemistry shapes contrasting concentration-discharge patterns. *Water. Resour. Res.* 55, 4233–4251.